Bacterial ecology and evolution converge on seasonal and decadal scales

Robin R. Rohwer[1*], Mark Kirkpatrick[1], Sarahi L. Garcia[2,3], Matthew Kellom[4], Katherine D. McMahon[5,6†], Brett J. Baker[1,7‡]

[1]The University of Texas at Austin, Department of Integrative Biology, 2415 Speedway #C0930, Austin, TX 78712, USA
[2]Carl von Ossietzky Universität Oldenburg, Institute for Chemistry and Biology of the Marine Environment (ICBM), 26129 Oldenburg, Germany
[3]Stockholm University, Department of Ecology, Environment, and Plant Sciences, Science for Life Laboratory, 106 91 Stockholm, Sweden
[4]DOE Joint Genome Institute, Lawrence Berkeley National Laboratory, 1 Cyclotron Road, Berkeley, CA 94720, USA
[5]University of Wisconsin-Madison, Department of Bacteriology, 1550 Linden Drive, Madison, WI, 53706, USA
[6]University of Wisconsin-Madison, Department of Civil and Environmental Engineering, 1550 Linden Drive, Madison, WI, 53706, USA
[7]The University of Texas at Austin, Department of Marine Science, Port Aransas, Austin, TX 78373, USA
Correspondence: *Robin.Rohwer@gmail.com, †trina.mcmahon@wisc.edu, and ‡brett_baker@utexas.edu

Ecology and evolution are distinct theories, but the short lifespans and large population sizes of microbes allow evolution to unfold along contemporary ecological time scales. To document this in a natural system, we collected a two-decade, 471-metagenome time series from a single site in a freshwater lake, which we refer to as the TYMEFLIES dataset. This massive sampling and sequencing effort resulted in the reconstruction of 30,389 metagenomic-assembled genomes (MAGs) over 50% complete, which dereplicated into 2,855 distinct genomes (>96% nucleotide sequence identity). We found both ecological and evolutionary processes occurred at seasonal time scales. There were recurring annual patterns at the species level in abundances, nucleotide diversities (π), and single nucleotide variant (SNV) profiles for the majority of all taxa. During annual blooms, we observed both higher and lower nucleotide diversity, indicating that both ecological differentiation and competition drove evolutionary dynamics. Overlayed upon seasonal patterns, we observed long-term change in 20% of the species' SNV profiles including gradual changes, step changes, and disturbances followed by resilience. Most abrupt changes occurred in a single species, suggesting evolutionary drivers are highly specific. Nevertheless, seven members of the abundant *Nanopelagicaceae* family experienced abrupt change in 2012, an unusually hot and dry year. This shift coincided with increased numbers of genes under selection involved in amino acid and nucleic acid metabolism, suggesting fundamental organic nitrogen compounds drive strain differentiation in the most globally abundant freshwater family. Overall, we observed seasonal and decadal trends in both interspecific ecological and intraspecific evolutionary processes. The convergence of microbial ecology and evolution on the same time scales demonstrates that understanding microbiomes requires a new unified approach that views ecology and evolution as a single continuum.

Main Text

Ecology and evolution are typically considered distinct processes that unfold on different time scales. Although microbial ecology has blossomed into a rich field spanning experimental and natural systems, our understanding of microbial evolution relies primarily on phylogenetic reconstructions and laboratory experiments. Phylogenies provide insight into ancient evolutionary events[1], but lack insight into contemporary evolution[2] that occurs on directly observable time scales. Laboratory approaches, such as the *E. coli* long-term evolution experiment[3], are able to directly observe evolutionary processes, but lack the context of complex communities typical of natural environments.

Here we describe a two-decade microbial time series from a freshwater lake, which allows us to directly observe the interplay between ecology and contemporary evolution in a natural ecosystem. We reconstructed tens of thousands of MAGs from 471 metagenomes spanning two decades with a sampling frequency averaging twice a month. This dataset constitutes the largest and longest metagenome dataset from a single location. We find that ecology and evolution both unfold at short, seasonal time scales as well as longer-term decadal time scales. The similar dynamics of inter- and intraspecies processes suggests that bacterial ecology and evolution unfold along a continuum that lacks a clear delineation between the two theories. We conclude that microbial ecology and evolution must be considered simultaneously and combined into a unified theory.

66 **The TYMEFLIES dataset**

67 We collected 471 samples over 20 years from Lake Mendota (WI, USA)[4] and obtained shotgun
68 DNA libraries (Fig. 1a, Supplementary Table 1). We refer to these Twenty Years of Metagenomes
69 Exploring Freshwater Lake Interannual Eco/evo Shifts as the TYMEFLIES dataset. By cross-
70 mapping reads from ~50 metagenomes to each single-sample metagenome assembly, we obtained
71 a total of 85,684 genome bins, 30,389 of which were medium or high quality (> 50% completeness
72 and < 10% contamination)[5]. We clustered these 30,389 bins at 96% average nucleotide identity
73 (ANI) and obtained 2,855 clusters from which we chose representative metagenome-assembled
74 genomes (MAGs)[6] (Supplementary Table 2). Several previous studies have found an emergent
75 species boundary at similar ANI cutoffs[7–9], and we observed a rapid increase in the number of
76 clusters above the 96% ANI cutoff. For the purposes of this study, we treat these 96% ANI
77 representative MAGs as bacterial species and refer to sub-species delineations as strains.

78

79 The representative MAGs have high estimated completeness (median 86%) and low contamination
80 (median 0.9%) (Fig. 1b), and reflect the lake's abundant bacterial community, especially in well-
81 sampled seasons (Fig. 1c). Using a 16S rRNA gene amplicon dataset from the same timeseries[4] as
82 a reference for the expected community composition (Fig. 1d), we found that our representative
83 MAGs comprise most of the abundant taxa (Fig. 1e). Moreover, we obtained 168 representative
84 MAGs from the *Nanopelagicales* order, which is the most abundant order in Lake Mendota and
85 accounts for 22% of the amplicon reads and 10% of the mapped metagenomic reads. Similar to
86 SAR11 bacteria in the oceans, this freshwater lineage is abundant in lakes globally[10], difficult to
87 culture[11], and typically has highly streamlined genomes[12].

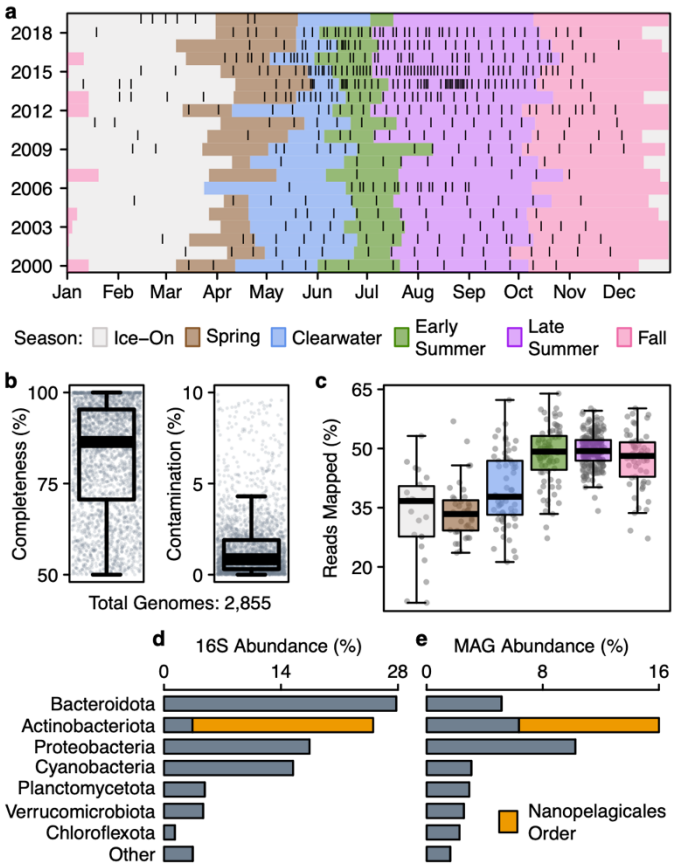

Fig. 1. The TYMEFLIES dataset. a, Metagenomes sample dates are indicated by black vertical lines. Microbial seasons[13] are indicated by colored shading. **b**, Quality of the 2,855 reference genomes obtained after clustering to 96% ANI. We treat these reference genomes as species. **c**, Percent of metagenome reads from each sample that mapped to all reference genomes with an ANI ≥ 93%. Samples are grouped by season to highlight how well the reference genomes reflect each seasonal community. **d**, Rank abundance of phyla as measured by 16S rRNA gene amplicon sequencing[4]. The abundant *Nanopelagicales* order of Actinobacteria is highlighted. **e**, Abundance of phyla in the TYMEFLIES reference genomes, quantified as the mean relative abundance normalized by genome size and sequencing depth. The *Nanopelagicales* order is again highlighted.

Seasonal ecology and evolution

Lake Mendota has been the focus of limnological research since the late 1800s and has been routinely sampled since 1984 by the North Temperate Lakes Long-Term Ecological Research program (NTL-LTER)[14]. Microbial sampling began in 2000 as part of an NSF microbial

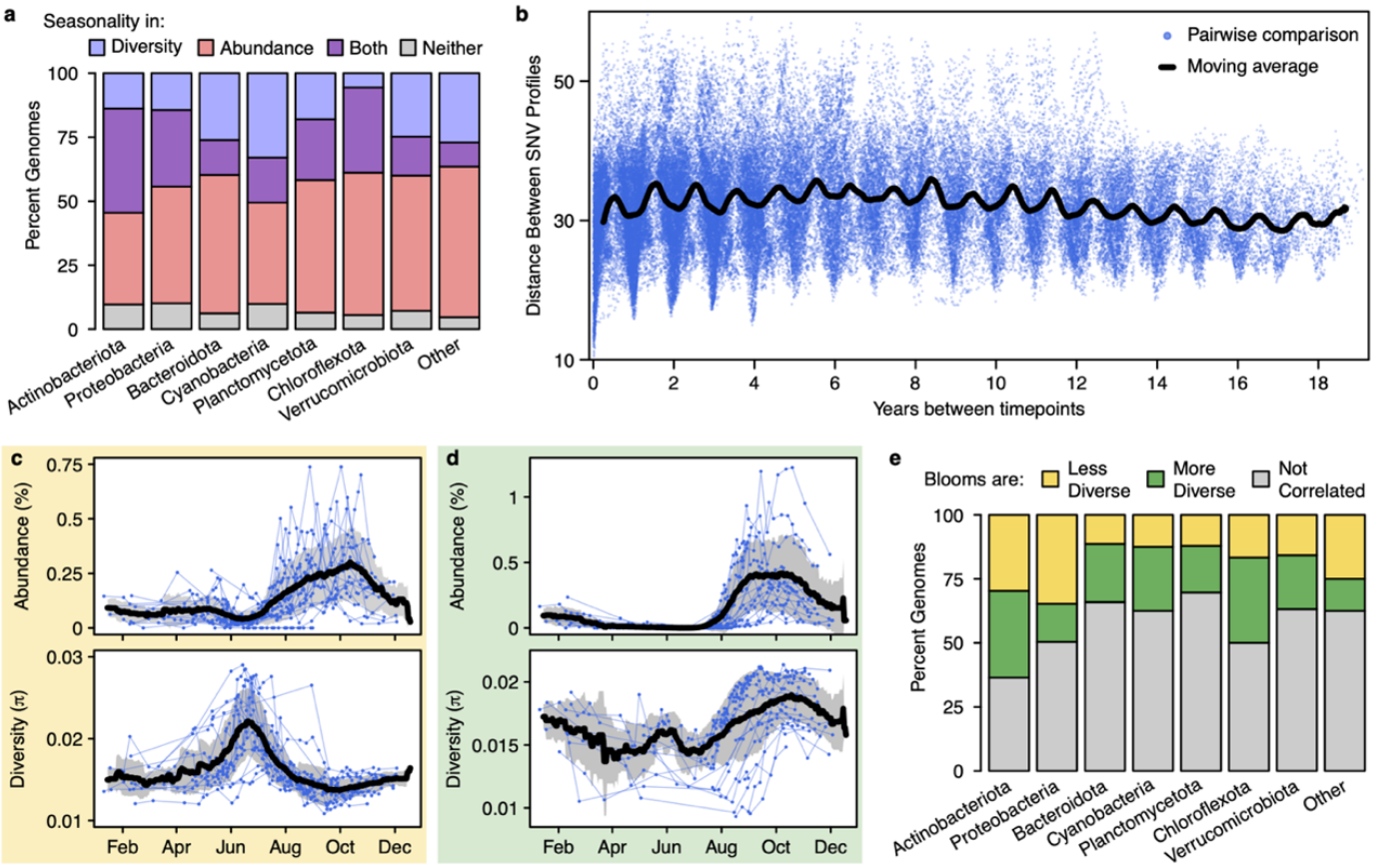

Fig. 2. Bacterial seasonality at the sub-species level. a, The percent of species with seasonality in nucleotide diversity and/or centered log ratio-transformed relative abundance. The 1,474 reference species that occurred at least 30 times were included in this analysis. **b**, A time decay plot of the Euclidean distances between the SNV profiles of an abundant species in the *Nanopelagicus* genus (ME2017-06-13_3300043469_group7_bin14). A more similar SNV profile indicates that the strain composition is more similar. Each blue point represents a pairwise comparison between two sample dates, with the time between those dates on the x-axis. The black line is a 6-month moving average, drawn to highlight the annual periodicity of strain similarities. **c**, An example of a "less diverse" bloom, where nucleotide diversity decreases as relative abundance increases. Displayed is an abundant species in the *Planktophila* genus (ME2011-09-04_3300044729_group3_bin142). **d**, An example of a "more diverse" bloom, where nucleotide diversity increases as abundance increases. Displayed is an abundant species in the *Nanopelagicaceae* family, MAG-120802 genus (ME2012-08-31_3300044613_group4_bin150). **e**, The distribution of bloom diversity patterns across the 365 species that had both seasonal abundance and seasonal nucleotide diversity.

observatory[15]. From this long history of research, we know the lake follows a consistent annual phenology, and that phenological patterns are changing in response to climate change and invasive species[16–19]. Rohwer *et. al*[13] found that these phenological dynamics extend to the bacterial community. To confirm that phenological abundance patterns also exist in our more finely resolved bacterial species, we identified annual peaks in species relative abundance using periodograms (magnitude of Fourier transforms). After limiting this temporal analysis to the subset of representative MAGs that occurred at least 30 times over at least 10 years, we found that 72% of these 1,474 bacterial species have consistent seasonal abundance patterns (Fig. 2a).

To determine whether evolutionary dynamics (*i.e.* changes in allele frequency within the population) also unfold seasonally, we mapped reads from each sample against each species' reference genome to identify shifts in strain composition evidenced by shifts in nucleotide diversity (π) and the profiles of single nucleotide variants (SNVs). We found that 33% of the same 1,474 species displayed consistent seasonal nucleotide diversity patterns (Fig. 2a). For a more granular view of strain composition, we created SNV profiles for each species where each date's profile consists of the percent reference base at each SNV position. After making our abundance cutoff more stringent by requiring a median coverage > 10x, we calculated the Euclidean distance between each sample's SNV profile for the most abundant 263 species. We found that 80% of these species had consistent phenological patterns in their strain composition (Fig. 2b). This demonstrates that phenological patterns evident in the bacterial community extend to the finest possible taxonomic resolution. Several short-term freshwater studies have also observed changes in strain composition on seasonal timescales[20,21]. Phenological patterns in sub-species strains

suggest that bacterial evolution, evidenced by intraspecific genomic change, also unfolds on seasonal timescales.

Given the ubiquity of seasonal patterns in both species abundance and sub-species diversity, we asked if they were correlated. We quantified whether a species' "bloom" in abundance consisted of fewer strains or more strains than its baseline composition. Of the 365 species with seasonal patterns in both abundance and nucleotide diversity (purple bars in Fig. 2a), we found both scenarios were common; 21% of these species had less diverse blooms (Fig. 2c and yellow bars in Fig. 2e), while 19% had more diverse blooms (Fig. 2d and green bars in Fig. 2e). Further, all abundant phyla demonstrated an even mix of both bloom types (Fig. 2e). A lower-diversity bloom suggests that a subset of strains outcompeted the others, while a higher-diversity bloom suggests that micro-niches allowed rarer strains to gain abundance, resulting in higher strain diversity due to a more even strain composition. This is in agreement with a previous study that found both overlapping and distinct niches within freshwater bacterial species[22]. The prevalence of both bloom diversity patterns highlights the lack of a clear boundary between ecological and evolutionary processes since identical intraspecific and interspecific processes are occurring simultaneously.

Long-term ecology and evolution

Long-term changes can be masked by seasonal oscillations, lost in what is referred to as the "invisible present"[23]. The unprecedented length of the TYMEFLIES metagenome dataset provides a unique lens into the invisible present, enabling the identification of overlayed long-term patterns.

To find long-term changes in SNV-based strain profiles, we developed a classifier trained on the distance between each date's SNV profile and the SNV profile of that species' first occurrence in the timeseries. We trained this classifier on 11 examples of manually identified temporal patterns, and then applied it to all 263 most abundant species. Our classifier identified gradual change (Fig. 3a), which may arise from genetic drift or in response to a slow press disturbance, as well as abrupt change (Fig 3b and c), which may arise if a disturbance reaches a tipping point threshold leading to a new stable state, or from a sudden environmental shift[24,25]. Among instances of abrupt change, we identified step changes (Fig. 3b), where the new strain composition persisted during the remainder of our time frame, as well as patterns of disturbance with resilience (Fig. 3c), where the strain composition recovered to baseline.

We found that 21% of the most abundant species experienced one kind of long-term change in their strain profiles during our 20-year study period, and these changes overlayed both seasonal and acyclical short-term dynamics (Fig. 3d). Abrupt change was almost twice as common as gradual change (36 vs. 19 species), and resilience was only slightly more common than a lasting step change (20 vs. 16 species) (Fig. 3d). The three long-term change patterns were found in many abundant species distributed across phyla (Fig. 3e). Many abundant Actinobacteriota species experienced long-term change. These long-term changes in SNV profiles reflect shifts in intraspecific strain composition, which is typically attributed to evolutionary processes. The fact that during our observation period over a fifth of the species experienced long-term changes in their strain profiles emphasizes the importance of including contemporary evolutionary change in our understanding of microbial ecology.

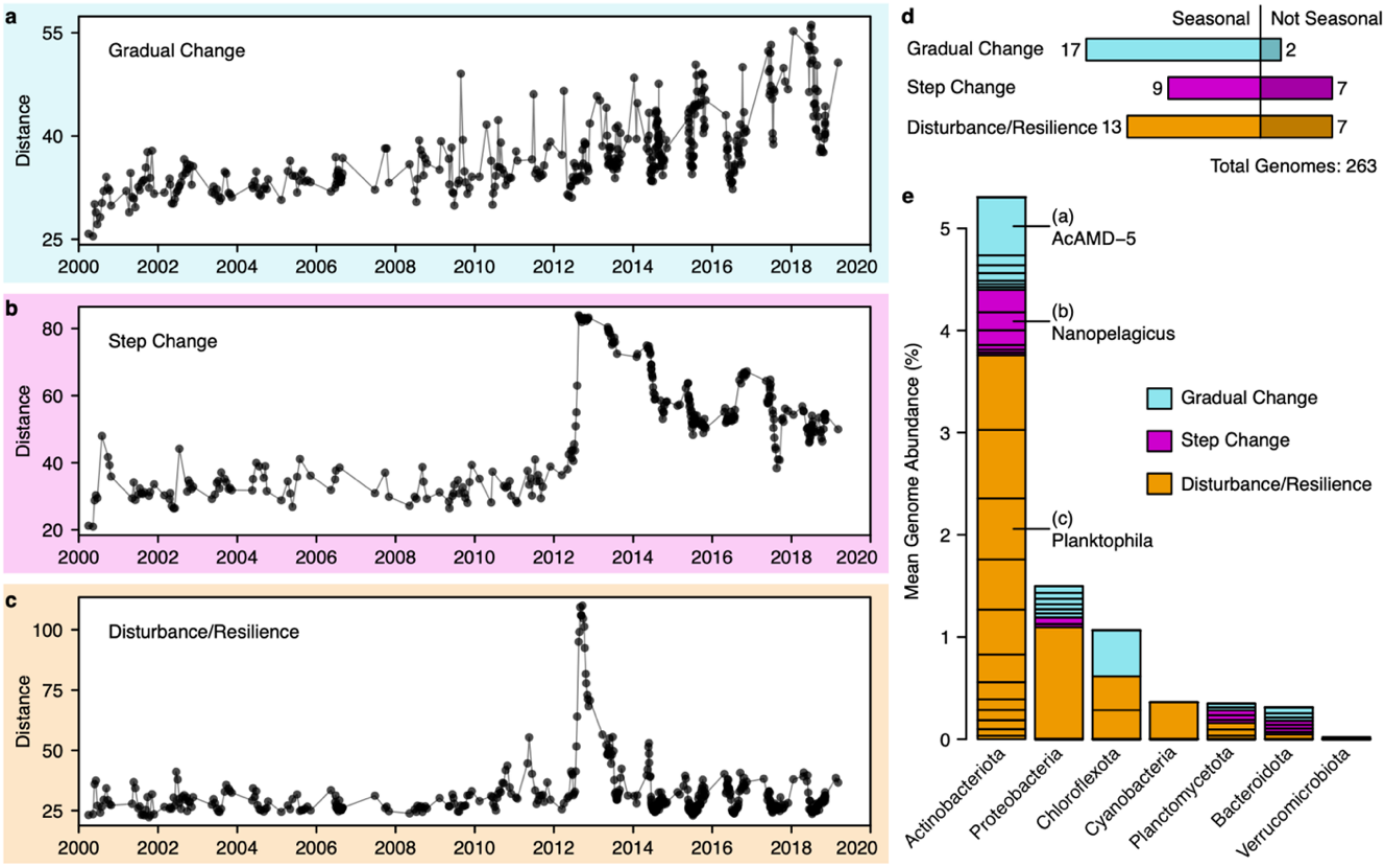

Fig. 3. Long-term changes in strain composition. a, An example of long-term, gradual change in strain composition. Points indicate sample dates, and distance refers to the Euclidean distance between a species' SNV profile on that sample date and that species' first available SNV profile. A species in the *Nanopelagicales* order, AcAMD-5 family is shown (ME2005-06-22_3300042363_group2_bin84). **b**, An example of an abrupt step change in strain composition in a species in the *Nanopelagicus* genus (ME2011-09-21_3300043464_group3_bin69). **c**, An example of a disturbance/resilience pattern, where an abrupt change in strain composition is followed by recovery to the original strain composition, in a species in the *Planktophila* genus (ME2015-07-03_3300042555_group6_bin161). **d**, Long-term change patterns often overlayed seasonal patterns. Of the 263 species abundant enough to observe their strain profiles, 39 had both long-term and seasonal patterns while 16 had only long-term patterns. **e**, The distribution of long-term patterns across phyla. Each species that underwent long-term change is indicated by a section of the phyla's bar, scaled by the mean abundance of that species. The sections corresponding to the examples highlighted in **a-c** are labelled.

Abrupt changes in *Nanopelagicaceae*

In general, related species did not change in unison with each other, suggesting that the drivers of evolutionary change are highly specific (Fig. 4a). One exception is an abrupt change event that impacted seven species in the *Nanopelagicaceae* (acI) family in 2012, specifically species in the *Nanopelagicus* and *Planktophila* genera (acI-B and acI-A). This is the most abundant family in Lake Mendota and in freshwaters globally[10], and the 127 *Nanopelagicaceae* reference species we recovered accounted for 8% relative abundance on average. Five of these *Nanopelagicaceae* species displayed resilience to the abrupt change, while two experienced lasting step changes in strain composition.

A myriad of possible environmental variables could have driven this event. A leading candidate is climate, which was unusually warm and dry in 2012. The lake experienced its highest epilimnion water temperatures since 1894[13] (Fig. 4b), the fifth shortest winter ice duration since 1856[26] (Fig. 4c), the 8th lowest annual discharge from its major tributary since 1976 and the second lowest peak discharge[27] (Fig. 4e). These climatic conditions led to top-down and bottom-up controls on the lake's primary productivity: the highest spring zooplankton abundance since measurements began in 1994[28] (Fig. 4d) was likely a result of the mild winter and spring allowing zooplankton populations, especially the prolific grazer *Daphnia pulicaria* to establish early, and low total phosphorus and soluble reactive phosphorus (Fig. 4f-g) was likely a result of low sediment transport associated with mild discharge events[29]. The resulting combination of high zooplankton grazing and low phosphorus, typically the limiting nutrient in lakes, may be responsible in turn for low phytoplankton biomass (Fig. 4h). Lake Mendota's dissolved organic

225 carbon (DOC) is primarily provided by phytoplankton[30], and consequently DOC was also low in

226 2012 (Fig. 4i).

227

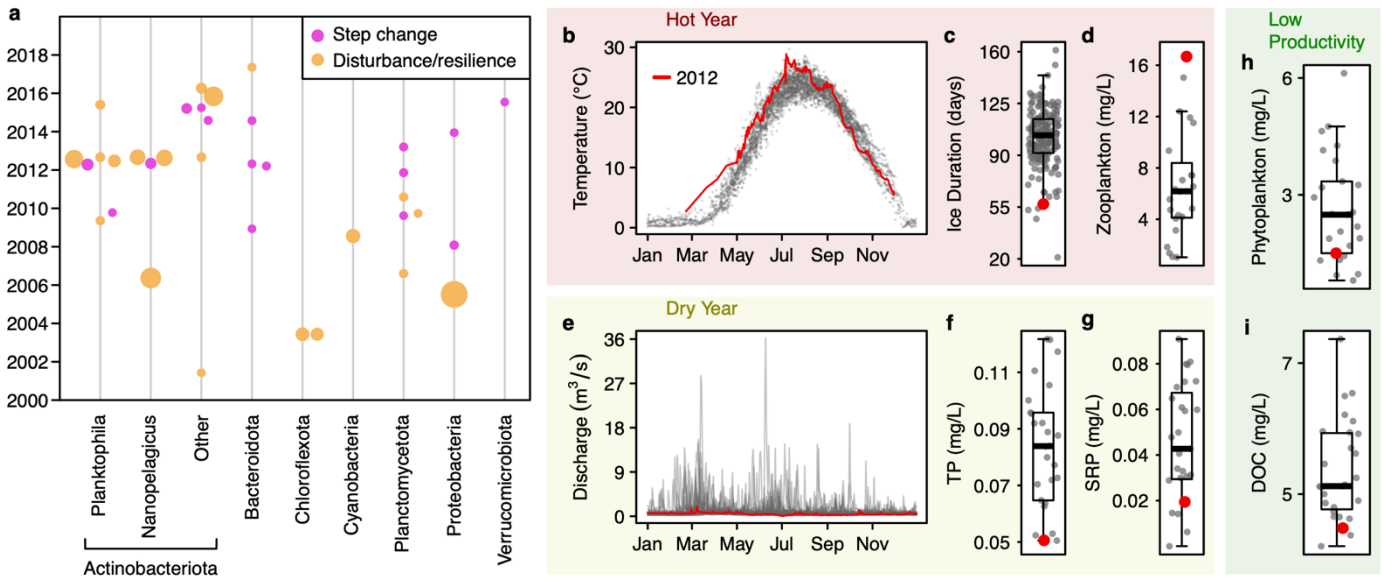

228

229 **Fig. 4. Abrupt changes in *Nanopelagicaceae* strain composition coincide with environmental**
230 **extremes in 2012. a**, Dates of all abrupt changes in strain composition arranged by phyla. Most
231 changes were isolated events, but multiple species from two abundant genera of Actinobacteriota,
232 *Planktophila* and *Nanopelagicus*, experienced abrupt change in 2012. Point size is scaled by
233 species abundance. **b**, Unusually high epilimnion water temperatures during spring and summer
234 2012 (relative to 1894 – 2019). **c**, The preceding winter had an unusually short ice duration
235 (relative to 1853 – 2023). **d**, Total zooplankton biomass (excluding predatory *Bythotrophes* and
236 *Leptodora*) was unusually high, likely enabled by warm early spring temperatures (relative to 1995
237 – 2018). **e**, Discharge from the Yahara River, the main tributary to Lake Mendota, was unusually
238 low and lacked high runoff events typical after storms and spring snowmelt (relative to 1989 -
239 2021). **f**, Sediment transport of total phosphorus, and **g**, of soluble reactive phosphorus were low
240 (relative to 1995 – 2021). **h**, Low phytoplankton biomass, likely resulting from both high
241 zooplankton grazing and low nutrient availability. **i**, Low dissolved organic carbon (relative to
242 1996 – 2022), likely a result of low phytoplankton abundance[30].

243

244 Another possible driver is the irruption of the invasive zooplankton spiny water flea (*Bythorephes*

245 *cedertrömii*) in 2009. This major disturbance resulted in a trophic cascade that decreased water

246 clarity[19,31], increased lake anoxia[28], and shifted the bacterial community composition[13]. Although

247 the abrupt changes in strain composition of seven *Nanopelagicaceae* species were observed three
248 years later, lag effects are common in complex ecosystems[32]. Ecosystem-wide drivers like the 2012
249 climate anomalies and the 2009 species invasion can have cascading and interacting effects on
250 nutrient and carbon dynamics, which in turn impact the bacterial community. The observed long-
251 term intraspecific changes suggest that such ecological drivers are also drivers of evolutionary
252 change, further emphasizing how ecology and evolution are intertwined.
253

254 **Evolutionary signals in a *Nanopelagicus***

255 To understand the dynamics of abrupt evolutionary change, we further examined one of the
256 abundant species, a *Nanopelagicus* (acI-B), that experienced a step change in strain composition
257 in August 2012 (Fig. 3b). An NMDS ordination of its SNV profiles indicated the strain composition
258 changed abruptly at that time and settled into a new composition after a period of adjustment in
259 2012 and 2013 (Fig. 5a).
260

261 The relative abundance of this species was quite constant throughout our 20-year observation
262 period (Fig. 5b), typically with higher abundances during the spring clearwater phase. The step
263 change in strain composition (Fig. 3b) coincided with one in nucleotide diversity (Fig. 5c). These
264 patterns could result from the spread of a new strain or with an increase in the evenness of
265 abundance in existing strains. To distinguish between these hypotheses, we counted the number
266 of previously unobserved SNVs in the mapped reads of every sample. We did not see large spikes
267 in new SNVs in 2012 (Fig. 5d), suggesting that the step changes reflected a shift in the relative
268 abundances of existing strains.
269

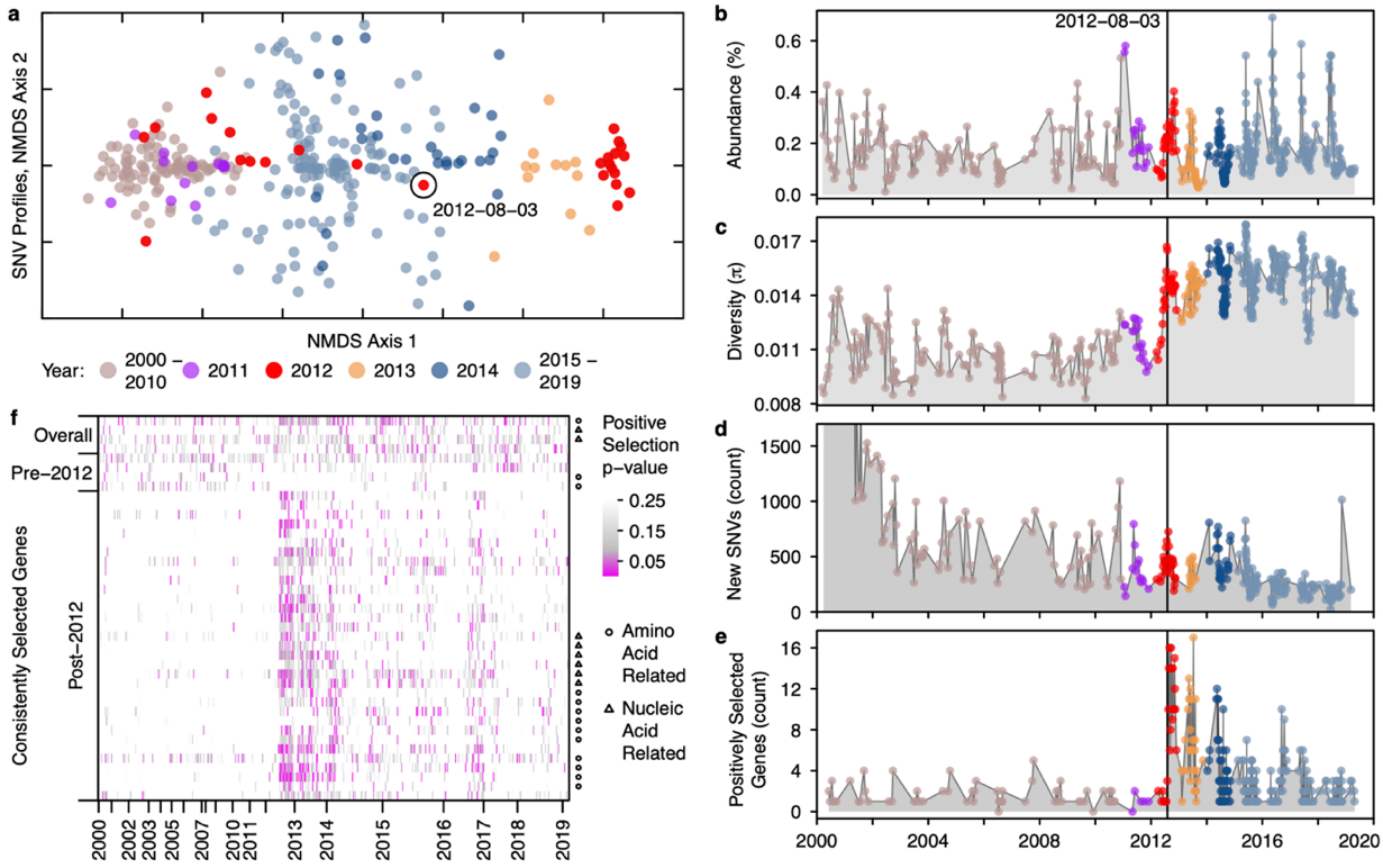

Fig. 5. Step change in strain composition coincides with more genes under selection. a, An abundant *Nanopelagicus* species experienced a step change in strain composition in 2012 (ME2011-09-21_3300043464_group3_bin69, see also Fig. 3b). Samples with more similar SNV profiles appear closer on this NMDS plot. Years 2000-2011 cluster together and are distinct from years 2014-2019, which cluster separately. A sudden change in strain composition occurred on August 3, 2012. **b**, Despite the abrupt change in strain composition, the relative abundance this species remained constant over time. **c**, Concurrent with the shift in strain composition, nucleotide diversity increased and then remained high, indicating that the new equilibrium was comprised of a more diverse assemblage of strains. **d**, The absence of a spike in the number of new SNVs suggests that an increase in the evenness of existing strains occurred, rather than the introduction of new strains. **e**, Concurrent with the shift in strain composition, the number of genes under positive selection also increased (McDonald-Kreitman F-statistic p-value < 0.05). **f**, Occurrence of consistently selected genes in all the samples, in the pre-2012 period, and in the post-2012 period. X-axis indicates samples over time and Y-axis indicates genes. Shading indicates the significance level of positive selection. Amino acid-related genes and nucleic acid-related genes are indicated on the right axis. Full annotations are available in Supplementary Table 3. Note that the X-axis is evenly spaced by sample, so that years with more samples take up more space.

289 This interpretation is consistent with a dramatic increase in the number of genes under positive
290 selection that occurred at this time (Fig. 5e). As the relative abundances of some strains increase,
291 alleles specific to them appear to undergo partial (or "soft") selective sweeps. As the strain
292 composition reequilibrates, this signal dies out (Fig 5e). To identify candidate loci that may be
293 important to adaptation that occurred during our sampling, we sought genes that consistently
294 showed signals of selection over the entire timeseries, only during the pre-2012 period, and only
295 during the post-2012 period. Four genes were consistently selected both pre- and post-2012, four
296 genes were consistently selected pre-2012, and 33 genes were consistently selected post-2012. We
297 used gene functional predictions[33] to identify their potential metabolic pathways. Of the 33
298 consistently selected genes post-2012, ten are involved in amino acid metabolism or
299 aminoacylation, and seven are involved with nucleic acid synthesis or degradation (Fig. 5f).
300
301 Previously, the absence of biosynthesis or auxotrophies for amino acids and nucleotides has been
302 highlighted for microorganisms with streamlined genomes[34,35]. In the streamlined *Nanopelagicus*,
303 auxotrophies for various amino acids[12,36] coupled with an enrichment of transporters for many
304 small organic nitrogen compounds, including amino acids[12,37,38] and nucleic acid components[12,36–
305 38] are common. Moreover, the histidine pathway was found split between two different strains of
306 *Nanopelagicus* growing in a mixed culture[36]. Our observation of consistent selection on amino
307 acid and nucleic acid metabolism suggests that these genes differentiate the post-2012 strains, thus
308 biosynthesis, use and reuse of small organic nitrogen compounds are key in the ecology and
309 evolution of these globally abundant lake bacteria.
310

A continuum of ecology and evolution

The interface between ecology and evolution is delineated by species boundaries, but in bacteria species concepts and definitions are hotly debated[39]. Using a commonly chosen definition for microbial species boundaries, we found processes that unfold as interspecies ecological dynamics also occur in intraspecies evolution. Moreover, the time scales of these processes overlapped, as did likely environmental drivers. How microbes will respond to global changes in land use, invasive species, and climate[40] are pressing questions that require an understanding of long-term change. Few microbial timeseries are long enough to capture such dynamics, but decadal observations are an essential approach to understand how complex ecosystems respond to global change. The two-decade TYMEFLIES dataset will serve as an invaluable community resource to continue addressing these questions and move us toward a unified approach to microbial ecology and evolution. Microbial ecology and evolution must be considered simultaneously and combined into a unified theory.

Methods

Data Availability

Metagenome sequences are available through the DOE Joint Genome Institute's Genome Portal under Proposal 504350 (https://genome.jgi.doe.gov/portal/Exttemetagenomes/Exttemetagenomes.info.html), and through the NCBI Sequence Read Archive at accessions listed in Supplementary Table 1. Reference MAG sequences are available through the NCBI GenBank IDs listed in Supplementary Table 2. Environmental data is publicly available through the Environmental Data Initiative

333 (https://edirepository.org/)[41–49] and the U.S. Geological Survey's Water Data for the Nation
334 (https://waterdata.usgs.gov/nwis)[27].
335

336 **Code Availability**

337 Custom scripts used for data processing are available at https://github.com/rrohwer/TYMEFLIES
338 and on Zenodo.
339

340 **Lake Mendota Samples**

341 Lake Mendota is a eutrophic temperate lake located in Madison, Wisconsin (USA). Integrated
342 epilimnion samples were collected from the upper 12 m at a 25 m deep location referred to as the
343 central "deep hole" (43°05'58.2"N 89°24'16.2"W). Bacteria were collected on 0.2 µm
344 polyethersulfone filters (Pall Corporation), stored at -80°C, and DNA was extracted after
345 randomizing sample order by a single person in 2018-2019 using FastDNA Spin Kits (MP
346 Biomedicals). A detailed description of the study site, sample collection, and DNA extraction
347 procedures is provided by Rohwer and McMahon[4].
348

349 **Metagenome sequencing and assembly**

350 Samples were sequenced by the US Department of Energy Joint Genome Institute (JGI) using a
351 NovaSeq 6000 with an S4 flow cell. Sample metadata is available in Supplementary Table 1, and
352 raw sequencing data is available through the JGI Genome Portal under Proposal 504350
353 (https://genome.jgi.doe.gov/portal/Exttemetagenomes/Exttemetagenomes.info.html), or from the
354 NCBI Sequence Read Archive under accession numbers listed in Supplementary Table 1. Read

355 filtering was performed using standard JGI protocols[50], which are additionally detailed as metadata
356 paired with each sample through the JGI IMG/M website. Briefly, BBDuk[51] was used to remove
357 adapters and quality trim reads, and BBMap[51] was used to identify and remove common
358 contaminants. In our analyses we treated the resulting filtered fastq files as the metagenome reads.
359 Single-sample assemblies were also generated by JGI with their standard protocol[50] using
360 metaSPAdes[52]. These filtered fastq files and paired single-sample assemblies are available through
361 the JGI Genome Portal under Proposal 504350.
362

363 **Obtaining and characterizing genomes**

364 Genomes were binned out of metagenomes using the Texas Advanced Computing Center's
365 Lonestar6 supercomputer. Metagenomic reads were mapped back to sample assemblies using
366 BBMap (version 38.22)[51], sorted BAM files were created using SAMtools (version 1.9)[53], and
367 metagenome-assembled genomes were binned using MetaBAT2 (version 2.12.1)[54]. Metagenomic
368 reads from different samples were cross-mapped back to each assembly. Cross-mapping scales
369 exponentially, so it was performed on assemblies and sample reads broken into approximately 50-
370 sample groups of consecutive sample dates, with samples from the same year grouped together.
371 This resulted in 85,684 genome bins. CheckM2 (version 0.1.3)[5] was used to asses bin quality,
372 including completeness and contamination estimates, and GTDB-tk (version 2.1.1)[55] was used to
373 assign GTDB taxonomy (release 207)[56] to all bins. 30,389 genome bins were at least 50% complete
374 and less than 10% contaminated, and these bins were de-replicated to 96% ANI using dRep
375 (version 3.4.0)[6]. To choose 96% as our ANI cutoff, we ran dRep at ANIs ranging from 90 to 99%
376 and examined the resulting number of de-replicated bins, as well as the number of bins from the

377 same assembly that were combined. We chose 96% ANI because very few (one) of the 30,389 bins
378 were combined into an ANI group with a bin created from the same assembly, and because 96%
379 ANI was generally located right before a sudden increase in the total number of genome groups.
380 Our goal was to separate as many species as possible, while combining strains that were so closely
381 related they would compete for mapped reads. Applying a 96% ANI cutoff with dRep resulted in
382 2,855 representative genomes, which we treated as species in this study.
383
384 To quantify the relative abundance of each species in every sample, we mapped all sample reads
385 against the concatenated 96% ANI reference genomes using bbmap (version 38.22)[51], created
386 sorted BAM files using SAMtools (version 1.9)[53], and calculated relative abundance using coverM
387 (version 0.6.1)[57]. With the coverM software, we required a minimum read percent identity of 93,
388 proper pairs only, and excluded 1000 bp from each contig end from the calculation. CoverM
389 calculates relative abundance as the mean coverage divided by the mean coverage across all
390 genomes multiplied by the proportion of reads that mapped to the genome, thus normalizing by
391 genome size to estimate the fraction of cells that belong to a given species in each sample. A table
392 of representative MAGs along with taxonomy annotations, quality statistics, and abundance
393 statistics is available as Supplementary Table 2.
394
395 To further characterize the genomes, we ran inStrain (version 1.7.1)[58] using a minimum read ANI
396 of 93%, as recommended by the inStrain documentation given our previous choice of 96% ANI to
397 dereplicate genomes. This software called SNVs and calculated nucleotide diversity, among other
398 metrics. To identify genes we ran prodigal (version 2.6.3)[59] on each genome separately. We then

399 used Kofamscan (version 1.3.0)[60] to assign gene annotations from the Kyoto Encyclopedia of
400 Genes and Genomes (KEGG) database (release 107.1)[33]. Additional custom analyses were
401 performed using the R programming language (version 4.1.2)[61], and relied extensively on the
402 data.table R package (version 1.14.8)[62], the lubridate R package (version 1.9.3)[63], and GNU
403 parallel (version 'Chandrayaan')[64].
404

405 **Classifying seasonal and long-term change**

406 To classify each species' abundance pattern as seasonal or not, we started with relative abundances
407 as calculated by coverM (version 0.6.1)[57] and further corrected any abundance to zero if the
408 genome's coverage breadth was 70% or less than its expected breadth, as calculated by inStrain
409 (version 1.7.1)[58]. We then applied a centered log ratio transformation to the relative abundance
410 values using the compositions R package (version 2.0-6)[65]. After taking a daily linear interpolation
411 to obtain evenly spaced samples, we detrended the temporal profiles with a cubic fit. Finally, we
412 performed a periodogram analysis by computing the magnitude of the fast Fourier transform. If a
413 peak occurred within 30 days of 365 days we considered it an annual oscillation, and if any of the
414 top five peaks corresponded to an annual period, we classified the species as having a seasonal
415 abundance pattern. We applied this analysis only to the 1,474 species that occurred on least 30
416 dates over at least 10 years. To classify each species' nucleotide diversity pattern as seasonal or
417 not, we similarly performed a fast Fourier transform on its inStrain-calculated nucleotide diversity
418 over time. We used the same periodogram analysis to classify it as having seasonal nucleotide
419 diversity or not, and we applied this analysis to the same subset of 1,474 species.
420

To characterize blooms as more diverse or less diverse, we calculated the Pearson correlation between centered log ratio-transformed relative abundance and nucleotide diversity for the 365 species that had both seasonal abundance and seasonal nucleotide diversity annual oscillations. We considered it a positive correlation (more diverse blooms) if the Pearson correlation was at least 0.35 and a negative correlation (less diverse blooms) if the Pearson correlation was less than or equal to -0.35. We repeated this analysis with up to two weeks of lag and used the highest correlation within that window. We chose 0.35 as a reasonable cutoff after manual examination of the first 150 species' correlations.

To calculate SNV profiles for each species, we created vectors corresponding to every SNV position in its genome, where the value of each element was the percent of mapped reads that matched the reference genome base at that position in each sample. SNV's were called using inStrain[58], and we only applied this analysis to samples where the species' median coverage was over 10x, as at coverages less than that we observed a drop in the total SNVs called. Therefore, for both long-term and seasonal analysis of SNV profiles, we included only species that had medium coverage over 10x on at least 30 dates over at least 10 years, which resulted in a subset of 263 species. To identify changes in SNV profiles, we created a distance matrix for each species based on Euclidean distances between each sample's SNV profile using the vegan R package (version 2.6-4)[66]. From this we created a table of time elapsed and Euclidean distance between each sample date.

To identify seasonal patterns in each species' SNV profiles, we created a daily linear interpolation of pairwise distances between all samples, taking the mean when multiple sample pairs occurred

with the same time interval. After detrending with a cubic fit, we performed a periodogram analysis to identify annual oscillations and the presence of seasonal patterns using the same criteria as with our abundance and nucleotide diversity annual oscillation analysis.

To identify long-term change patterns, we subset our pairwise distance table to the distance of each sample from the first sample. We developed a classifier for these temporal profiles of distances between SNV profiles using 11 manually chosen species. Our classifier criteria was hierarchical: first gradual change was identified, then step change was identified, and finally disturbance/resilience patterns were identified. After training, the classifier was applied to all 263 species above the abundance cutoff. Gradual change was identified if a linear fit to the daily linearly interpolated distances, excluding dates closer than a month to the starting date, resulted in an adjusted R^2 of at least 0.55. Dates closer than a month to the starting date were excluded because they tended to be highly similar, and a linear interpolation was applied to account for uneven sampling dates, particularly the high frequency of summer sampling in the latter decade of the timeseries. Possible step change locations were identified after excluding dates closer than a month to the starting date and applying an F test to the linearly interpolated distances using the strucchange R package (version 1.5-3)[67]. If a breakpoint was identified by the F test, the means of measured (as opposed to interpolated) before and after distances were different (Mann-Whitnes p-value < 0.01), and the step resulted in a new mean at least 33% higher than the previous mean, a step change pattern was identified. Disturbance/resilience patterns were then identified using outlier distances calculated by the default boxplot statistics in R. If a date's distance was > 1.5 times the difference between the 3rd and 1st quartile of observed distances a date was considered

466 an outlier, and if outlier values were maintained for at least a month the species was classified as
467 having a disturbance event with resilience.
468

469 **Analyzing abrupt change in *Nanopelagicaceae***

470 To place environmental conditions in 2012 in context, historical environmental data was collected
471 from the North Temperate Lakes Long-Term Ecological Research program (NTL-LTER) through
472 the Environmental Data Initiative (EDI) interface (https://edirepository.org/) and the US
473 Geological Survey (USGS) Water Data for the Nation (https://waterdata.usgs.gov/nwis) using the
474 USGS dataRetrieval R package (version 2.7.14)[68]. EDI datasets analyzed included ice duration[26];
475 nutrients, pH, and carbon[41]; major ions[42]; water temperatures combined from multiple datasets[45–
476 49] as described in Rohwer *et al.*[13]; phytoplankton[43]; and zooplankton[44] converted to biomass as
477 described in Rohwer, Ladwig, *et al.*[28]. River discharge measurements were obtained from the
478 USGS for the Yahara River, the primary tributary into Lake Mendota (site ID: 05427718)[27]. After
479 exploring all parameters included in these datasets, the occurrence of a hot, dry year with low
480 primary productivity became apparent.
481

482 Relative abundance and nucleotide diversity of the *Nanopelagicus* MAG ME2011-09-
483 21_3300043464_group3_bin69 were calculated as for the seasonal analysis. New SNVs were
484 identified as SNV positions that were called by inStrain[58] for the first time in a given sample.
485 Genes under selection were identified using dN/dS and pN/pS ratios as calculated by inStrain[58]. A
486 McDonald-Kreitman test[69] was used to identify positively selected genes where the bias of unfixed
487 SNVs to be nonsynonymous was lower than the bias of fixed SNVs to be nonsynonymous

488 (pNpS/dNdS < 1), and positive selection was considered statistically significant when the Fisher
489 p-value was less than or equal to 0.05. A gene was considered consistently selected if it appeared
490 under significant positive selection with high frequency (in the 4th quartile). Consistently selected
491 genes were identified for the pre-2012 and post-2012 time periods separately.
492
493 Gene annotations were analyzed in the context of the KEGG pathways[33] they belonged to. For
494 each potential pathway, all genes present in the genome were visualized with KEGG Pathway
495 Maps (https://www.genome.jp/brite/br08901). When multiple genes that surrounded the selected
496 gene existed in the genome, that pathway was considered a likely annotation. When likely
497 pathways involved amino acid metabolism or aminoacylation, they were considered amino acid-
498 related. When likely pathways involved purine or pyrimidine metabolism, they were considered
499 nucleic acid-related.
500

501 **References**

502 1. Hug, L. A. *et al.* A new view of the tree of life. *Nature Microbiology* **1**, (2016).
503 2. Brennan, G. L. & Logares, R. Tracking contemporary microbial evolution in a changing ocean.
504 *Trends in Microbiology* **31**, 336–345 (2023).
505 3. Lenski, R. E. Experimental evolution and the dynamics of adaptation and genome evolution in
506 microbial populations. *ISME J* **11**, 2181–2194 (2017).
507 4. Rohwer, R. R. & McMahon, K. D. Lake iTag measurements over nineteen years, introducing
508 the limony dataset. 2022.08.04.502869 Preprint at https://doi.org/10.1101/2022.08.04.502869
509 (2022).

510 5. Chklovski, A., Parks, D. H., Woodcroft, B. J. & Tyson, G. W. CheckM2: a rapid, scalable and
511 accurate tool for assessing microbial genome quality using machine learning.
512 2022.07.11.499243 Preprint at https://doi.org/10.1101/2022.07.11.499243 (2022).
513 6. Olm, M. R., Brown, C. T., Brooks, B. & Banfield, J. F. dRep: a tool for fast and accurate
514 genomic comparisons that enables improved genome recovery from metagenomes through de-
515 replication. *ISME J* **11**, 2864–2868 (2017).
516 7. Varghese, N. J. *et al.* Microbial species delineation using whole genome sequences. *Nucleic*
517 *Acids Research* **43**, 6761–6771 (2015).
518 8. Jain, C., Rodriguez-R, L. M., Phillippy, A. M., Konstantinidis, K. T. & Aluru, S. High
519 throughput ANI analysis of 90K prokaryotic genomes reveals clear species boundaries. *Nat*
520 *Commun* **9**, 1–8 (2018).
521 9. Olm, M. R. *et al.* Consistent Metagenome-Derived Metrics Verify and Delineate Bacterial
522 Species Boundaries. *mSystems* **5**, 10.1128/msystems.00731-19 (2020).
523 10. Lipko, I. A. & Belykh, O. I. Environmental Features of Freshwater Planktonic Actinobacteria.
524 *Contemp. Probl. Ecol.* **14**, 158–170 (2021).
525 11. Kim, S., Kang, I., Seo, J.-H. & Cho, J.-C. Culturing the ubiquitous freshwater actinobacterial
526 acI lineage by supplying a biochemical 'helper' catalase. *ISME J* **13**, 2252–2263 (2019).
527 12. Neuenschwander, S. M., Ghai, R., Pernthaler, J. & Salcher, M. M. Microdiversification in
528 genome-streamlined ubiquitous freshwater Actinobacteria. *ISME J* **12**, 185–198 (2018).
529 13. Rohwer, R. R., Hale, R. J., Vander Zanden, M. J., Miller, T. R. & McMahon, K. D. Species
530 invasions shift microbial phenology in a two-decade freshwater time series. *Proceedings of the*
531 *National Academy of Sciences* **120**, e2211796120 (2023).

14. Magnuson, J. J., Kratz, T. K. & Benson, B. J. *Long-Term Dynamics of Lakes in the Landscape: Long-Term Ecological Research on North Temperate Lakes*. (Oxford University Press, 2006).

15. Yannarell, A. C., Kent, A. D., Lauster, G. H., Kratz, T. K. & Triplett, E. W. Temporal Patterns in Bacterial Communities in Three Temperate Lakes of Different Trophic Status. *Microb Ecol* **46**, 391–405 (2003).

16. Magee, M. R. & Wu, C. H. Effects of changing climate on ice cover in three morphometrically different lakes. *Hydrol. Process.* **31**, 308–323 (2017).

17. Magee, M. R. & Wu, C. H. Response of water temperatures and stratification to changing climate in three lakes with different morphometry. *Hydrology and Earth System Sciences* **21**, 6253–6274 (2017).

18. Snortheim, C. A. *et al.* Meteorological drivers of hypolimnetic anoxia in a eutrophic, north temperate lake. *Ecological Modelling* **343**, 39–53 (2017).

19. Matsuzaki, S.-I. S. *et al.* Climate and food web effects on the spring clear-water phase in two north-temperate eutrophic lakes. *Limnol. Oceanogr.* **n/a**, 1–17 (2020).

20. Okazaki, Y., Nakano, S., Toyoda, A. & Tamaki, H. Long-Read-Resolved, Ecosystem-Wide Exploration of Nucleotide and Structural Microdiversity of Lake Bacterioplankton Genomes. *mSystems* **7**, e00433-22 (2022).

21. Meziti, A. *et al.* Quantifying the changes in genetic diversity within sequence-discrete bacterial populations across a spatial and temporal riverine gradient. *The ISME Journal* **13**, 767 (2019).

22. Garcia, S. L. *et al.* Contrasting patterns of genome-level diversity across distinct co-occurring bacterial populations. *The ISME Journal* 1 (2017) doi:10.1038/s41396-017-0001-0.

23. Magnuson, J. J. Long-Term Ecological Research and the Invisible Present. *BioScience* **40**, 495–501 (1990).

24. Turner, M. G. *et al.* Climate change, ecosystems and abrupt change: science priorities. *Philosophical Transactions of the Royal Society B: Biological Sciences* **375**, 20190105 (2020).

25. Scheffer, M., Carpenter, S., Foley, J. A., Folke, C. & Walker, B. Catastrophic shifts in ecosystems. *Nature* **413**, 591–596 (2001).

26. Magnuson, J. J., Carpenter, S. R. & Stanley, E. H. North Temperate Lakes LTER: Ice Duration - Madison Lakes Area 1853 - current. Environmental Data Initiative https://doi.org/10.6073/PASTA/69B3391E13955392587413ECBFC7C298 (2023).

27. U.S. Geological Survey National Water Information System data available on the World Wide Web. USGS 05427718 Yahara River at Windsor, WI, Daily Discharge 00060. U.S. Geological Survey National Water Information System data available on the World Wide Web (2023).

28. Rohwer, R. R. *et al.* Increased anoxia following species invasion of a eutrophic lake. *Limnology and Oceanography Letters* **n/a**, (2023).

29. Carpenter, S. R., Booth, E. G. & Kucharik, C. J. Extreme precipitation and phosphorus loads from two agricultural watersheds. *Limnology and Oceanography* **63**, 1221–1233 (2018).

30. Berg, S. M., Peterson, B. D., McMahon, K. D. & Remucal, C. K. Spatial and Temporal Variability of Dissolved Organic Matter Molecular Composition in a Stratified Eutrophic Lake. *Journal of Geophysical Research: Biogeosciences* **127**, e2021JG006550 (2022).

31. Walsh, J. R., Carpenter, S. R. & Zanden, M. J. V. Invasive species triggers a massive loss of ecosystem services through a trophic cascade. *PNAS* **113**, 4081–4085 (2016).

32. Rastetter, E. B. *et al.* Time lags: insights from the U.S. Long Term Ecological Research Network. *Ecosphere* **12**, e03431 (2021).

578 33. Kanehisa, M., Furumichi, M., Sato, Y., Kawashima, M. & Ishiguro-Watanabe, M. KEGG for
579 taxonomy-based analysis of pathways and genomes. *Nucleic Acids Research* **51**, D587–D592
580 (2023).
581 34. Ramoneda, J., Jensen, T. B. N., Price, M. N., Casamayor, E. O. & Fierer, N. Taxonomic and
582 environmental distribution of bacterial amino acid auxotrophies. *Nat Commun* **14**, 7608 (2023).
583 35. Castelle, C. J. *et al.* Biosynthetic capacity, metabolic variety and unusual biology in the CPR
584 and DPANN radiations. *Nat Rev Microbiol* **16**, 629–645 (2018).
585 36. Garcia, S. L. *et al.* Auxotrophy and intrapopulation complementary in the 'interactome' of a
586 cultivated freshwater model community. *Mol Ecol* **24**, 4449–4459 (2015).
587 37. Garcia, S. L. *et al.* Metabolic potential of a single cell belonging to one of the most abundant
588 lineages in freshwater bacterioplankton. *The ISME Journal* **7**, 137 (2013).
589 38. Hamilton, J. J. *et al.* Metabolic Network Analysis and Metatranscriptomics Reveal
590 Auxotrophies and Nutrient Sources of the Cosmopolitan Freshwater Microbial Lineage acI.
591 *MSystems* **2**, e00091-17 (2017).
592 39. Rosselló-Móra, R. & Amann, R. Past and future species definitions for Bacteria and Archaea.
593 *Systematic and Applied Microbiology* **38**, 209–216 (2015).
594 40. Tiedje, J. M. *et al.* Microbes and Climate Change: a Research Prospectus for the Future. *mBio*
595 e00800-22 (2022) doi:10.1128/mbio.00800-22.
596 41. Magnuson, J. J., Carpenter, S. R. & Stanley, E. H. North Temperate Lakes LTER: Chemical
597 Limnology of Primary Study Lakes: Nutrients, pH and Carbon 1981 - current. Environmental
598 Data Initiative https://doi.org/10.6073/PASTA/325232E6E4CD1CE04025FA5674F7B782
599 (2023).

42. Magnuson, J. J., Carpenter, S. R. & Stanley, E. H. North Temperate Lakes LTER: Chemical Limnology of Primary Study Lakes: Major Ions 1981 - current. Environmental Data Initiative https://doi.org/10.6073/pasta/bb563f16c7338fdb3ddf82057ef43cc6 (2023).

43. Magnuson, J. J., Carpenter, S. R. & Stanley, E. H. North Temperate Lakes LTER: Phytoplankton - Madison Lakes Area 1995 - current. Environmental Data Initiative https://doi.org/10.6073/PASTA/43D3D401AF88CC05C6595962BDB1AB5C (2022).

44. Magnuson, J., Carpenter, S. & Stanley, E. North Temperate Lakes LTER: Zooplankton - Madison Lakes Area 1997 - current. Environmental Data Initiative https://doi.org/10.6073/PASTA/D5ABE9009D7F6AA87D1FCF49C8C7F8C8 (2022).

45. Rohwer, R. R. & McMahon, K. D. Lake Mendota Microbial Observatory Temperature, Dissolved Oxygen, pH, and conductivity data, 2006-present. Environmental Data Initiative https://doi.org/10.6073/PASTA/7E533C197ED8EBD27777A89A2C8D7DFE (2022).

46. Magnuson, J. J., Carpenter, S. R. & Stanley, E. H. North Temperate Lakes LTER: Physical Limnology of Primary Study Lakes 1981 - current. Environmental Data Initiative https://doi.org/10.6073/PASTA/316203040EA1B8ECE89673985AB431B7 (2021).

47. Magnuson, J., Carpenter, S. & Stanley, E. North Temperate Lakes LTER: High Frequency Water Temperature Data - Lake Mendota Buoy 2006 - current. Environmental Data Initiative https://doi.org/10.6073/PASTA/8CEFF296AD68FA8DA6787076E0A5D992 (2020).

48. Robertson, D. Lake Mendota water temperature secchi depth snow depth ice thickness and meterological conditions 1894 - 2007. Environmental Data Initiative https://doi.org/10.6073/PASTA/F20F9A644BD12E4B80CB288F1812C935 (2016).

621 49. Magnuson, J. J., Carpenter, S. R. & Stanley, E. H. Lake Mendota Multiparameter Sonde
622 Profiles: 2017 - current. Environmental Data Initiative
623 https://doi.org/10.6073/PASTA/5F15BF453851987FC030B2F07A110B21 (2021).
624 50. Clum, A. *et al.* DOE JGI Metagenome Workflow. *mSystems* **6**, 10.1128/msystems.00804-20
625 (2021).
626 51. Bushnell, B. *BBMap Short Read Aligner and Other Bioinformatic Tools*.
627 https://www.osti.gov/biblio/1241166 (2014).
628 52. Nurk, S., Meleshko, D., Korobeynikov, A. & Pevzner, P. A. metaSPAdes: a new versatile
629 metagenomic assembler. *Genome Res* **27**, 824–834 (2017).
630 53. Li, H. *et al.* The Sequence Alignment/Map format and SAMtools. *Bioinformatics* **25**, 2078–
631 2079 (2009).
632 54. Kang, D. D. *et al.* MetaBAT 2: an adaptive binning algorithm for robust and efficient genome
633 reconstruction from metagenome assemblies. *PeerJ* **7**, e7359 (2019).
634 55. Chaumeil, P.-A., Mussig, A. J., Hugenholtz, P. & Parks, D. H. GTDB-Tk: a toolkit to classify
635 genomes with the Genome Taxonomy Database. *Bioinformatics* btz848 (2019)
636 doi:10.1093/bioinformatics/btz848.
637 56. Parks, D. H. *et al.* GTDB: an ongoing census of bacterial and archaeal diversity through a
638 phylogenetically consistent, rank normalized and complete genome-based taxonomy. *Nucleic*
639 *Acids Research* **50**, D785–D794 (2022).
640 57. Aroney, S. T. N. *et al.* CoverM: Read coverage calculator for metagenomics. Zenodo
641 https://doi.org/10.5281/zenodo.10531254 (2024).
642 58. Olm, M. R. *et al.* inStrain profiles population microdiversity from metagenomic data and
643 sensitively detects shared microbial strains. *Nat Biotechnol* **39**, 727–736 (2021).

59. Hyatt, D. *et al.* Prodigal: prokaryotic gene recognition and translation initiation site identification. *BMC Bioinformatics* **11**, 119 (2010).

60. Aramaki, T. *et al.* KofamKOALA: KEGG Ortholog assignment based on profile HMM and adaptive score threshold. *Bioinformatics* **36**, 2251–2252 (2020).

61. R Core Team. *R: A Language and Environment for Statistical Computing*. (R Foundation for Statistical Computing, Vienna, Austria, 2022).

62. Barrett, T. *et al. Data.Table: Extension of `data.Frame`*. (2024).

63. Grolemund, G. & Wickham, H. Dates and Times Made Easy with lubridate. *Journal of Statistical Software* **40**, 1–25 (2011).

64. Tange, O. GNU Parallel 20230822 ('Chandrayaan'). Zenodo https://doi.org/10.5281/zenodo.8278274 (2023).

65. Boogaart, K. G. van den, Tolosana-Delgado, R. & Bren, M. compositions: Compositional Data Analysis. (2023).

66. Oksanen, J. *et al.* vegan: Community Ecology Package. (2022).

67. Zeileis, A. *et al.* strucchange: Testing, Monitoring, and Dating Structural Changes. (2022).

68. DeCicco, L., Hirsch, R., Lorenz, D., Watkins, D. & Johnson, M. *dataRetrieval: R Packages for Discovering and Retrieving Water Data Available from U.S. Federal Hydrologic Web Services*. (U.S. Geological Survey, Reston, VA, 2023). doi:10.5066/P9X4L3GE.

69. McDonald, J. H. & Kreitman, M. Adaptive protein evolution at the Adh locus in Drosophila. *Nature* **351**, 652–654 (1991).

Acknowledgements

Long-term datasets such as TYMEFLIES rely on researchers who contribute a portion of their time and effort to future projects. This work would not be possible without the generosity of many, including Lake Mendota sampling leads Angela Kent, Tony Yannarell, Ashley Shade, Stuart Jones, Ryan Newton, Georgia Wolfe, Emily Kara Read, Lucas Beversdorf, James Mutschler, and the original Microbial Observatory lead Eric W. Triplett. We thank Peter Golightly for his advice on interpreting the genes under selection data.

Funding

This project was supported by an E. Michael and Winona Foster WARF Wisconsin Idea Fellowship (R.R.R.), the U.S. National Science Foundation (NSF) (DBI-2011002) (R.R.R.), the U.S. National Institutes of Health (RO1-GM116853) (M.Kirk.), the U.S. NSF (DEB-1831730) (M. Kirk.), the U.S. Department of Agriculture (WIS01516 and WIS01789) (K.D.M.), the U.S. NSF (DEB-0702395, DEB-1344254) (K.D.M.) and a Simons Foundation Investigator in Aquatic Microbial Ecology Award (LI-SIAME-00002001) (B.J.B.). Support for sampling was provided by the U.S. NSF North Temperate Lakes Long-Term Ecological Research program (DEB-9632853, DEB-0217533, DEB-0822700, DEB-1440297, DEB-2025982) and the U.S. NSF Microbial Observatory program (MCB-9977903, DEB-0702395). The work (proposal: https://doi.org/10.46936/10.25585/60001198) conducted by the U.S. Department of Energy Joint Genome Institute (https://ror.org/04xm1d337), a DOE Office of Science User Facility, is supported by the Office of Science of the U.S. Department of Energy operated under Contract No. DE-AC02-05CH11231. The authors acknowledge the Texas Advanced Computing Center (TACC) at The

University of Texas at Austin for providing HPC resources that have contributed to the research results reported within this paper (http://www.tacc.utexas.edu).

Author Contributions

R.R.R. and K.D.M. conceptualized the research and obtained initial funding. K.D.M. and B.J.B. provided resources. R.R.R. conducted field and laboratory work and curated data. RRR performed analyses and created visualizations. M.Kirk. advised statistical approaches. S.L.G., M.Kell.., K.D.M., and B.J.B. advised analysis approaches. R.R.R. wrote the first draft, and R.R.R. and B.J.B. wrote the final draft incorporating edits provided by M.Kirk., S.L.G., M.Kell., and K.D.M.

Competing Interests

The authors declare no competing interests.

Supplemental Information

Supplementary Table 1. TYMEFLIES sample metadata. All the JGI, GOLD, NCBI, and internal McMahon Lab identifiers that pair with each metagenome sample.

Supplementary Table 2. TYMEFLIES reference genome metadata. NCBI identifiers corresponding to each reference genome, as well as the quality results from CheckM2[5], the taxonomy results from GTDB-tk[55], and average relative abundances as calculated by coverM[57].

Supplementary Table 3. Consistently selected gene annotations. KEGG annotations of consistently selected genes. Table row order matches heatmap row order in Fig. 5f.